ORNL/TM-2024/3254

Evaluating Optical Techniques to Characterize Solid-State Samples for the Plutonium-238 Supply Program

Luke R. Sadergaski
Hunter B. Andrews
Jeffrey Sharpe
Kristian G. Myhre
Adam J. Parkison

January 2024

OAK RIDGE National Laboratory

ORNL IS MANAGED BY UT-BATTELLE LLC FOR THE US DEPARTMENT OF ENERGY

ORNL/TM-2024/3254

Radioisotope Science and Technology Division

EVALUATING OPTICAL TECHNIQUES TO CHARACTERIZE SOLID-STATE SAMPLES FOR THE PLUTONIUM-238 SUPPLY PROGRAM

Luke R. Sadergaski
Hunter B. Andrews
Jeffrey Sharpe
Kristian G. Myhre
Adam J. Parkison

January 2024

Prepared by
OAK RIDGE NATIONAL LABORATORY
Oak Ridge, TN 37831-6283
managed by
UT-BATTELLE, LLC
for the
US DEPARTMENT OF ENERGY
under contract DE-AC05-00OR22725

CONTENTS

LIST OF FIGURES

ABBREVIATIONS

CCD	charge coupled device
DR	diffuse reflectance
DRS	diffuse reflectance spectroscopy
GSR	gunshot residue
ICCD	intensified charge coupled device
LIBS	laser-induced breakdown spectroscopy
MDD	modified direct denitration
MSF	microscope slide fixture
NIR	near-infrared
ORNL	Oak Ridge National Laboratory
PC	principal component
PCA	principal component analysis
pXRD	powder x-ray diffraction
R&D	research and development
RCT	Radiological control technician
REDC	Radioisotope Engineering Development Center
SEM	scanning electron microscopy
SIMCA	Soft Independent Modeling of Class Analogy
UV	ultraviolet
Vis	visible

ACKNOWLEDGMENTS

Funding for this program was provided by the National Aeronautics and Space Administration's Science Mission Directorate and administered by the US Department of Energy Office of Nuclear Energy under contract DEAC05-00OR22725. This work used resources at the High Flux Isotope Reactor, a US Department of Energy Office of Science User Facility operated by Oak Ridge National Laboratory.

ABSTRACT

This report documents steps that have been taken to establish advanced characterization capabilities for solid-state samples to support the ^{238}Pu Supply Program. The program has already invested significantly in spectroscopy and online monitoring development for liquid processes. Many of the data, analytical methods, and equipment could also be leveraged for the analysis of Np/Pu oxides and Np pellets to help classify material properties and link them to operations. The techniques described in this work include diffuse reflectance spectroscopy (DRS), Raman spectroscopy, and laser-induced breakdown spectroscopy (LIBS). Each technique is sensitive to various chemical and/or elemental species and can provide complimentary information to more standard methods such as powder x-ray diffraction and scanning electron microscopy. These options are remotely deployable via fiber-optic cables. DRS and Raman spectroscopy are already approved for glove box and hot cell work, but LIBS requires US Department of Energy approval for incorporation. Raman spectroscopy does require laser shielding, which means that DRS is the easiest method to implement. However, each technique provides complimentary data, and the most robust sample characterization could be achieved when all three, among other methods, are harnessed together. This report documents some of the progress made testing these capabilities, some of the challenges, and next steps to optimize the technology and integration strategies.

1. BACKGROUND AND MOTIVATION

1.1 INTRODUCTION

Spectrophotometry is an important component of the ^{238}Pu Supply Program for measuring Np and Pu concentrations, oxidation state(s), and monitoring separations.[1–19] Spectrophotometry, or *absorption spectroscopy*, is a technique that quantifies the amount of light absorbed by a sample as a function of wavelength. Ultraviolet (UV)–visible (Vis)–near-infrared (NIR) spectrometers collect spectra at relatively rapid intervals (e.g., 10–1,000 ms) and contain a wealth of information. Multivariate regression models can be used to convert spectra into concentrations for timely analytical measurements in glove box and hot cell environments at the Radioisotope Engineering Development Center (REDC). Fiber-optic cables transmit light to enable in situ UV-Vis-NIR absorption measurements while personnel operate equipment in a control room (Figure 1.1). Remote measurements directly in the hot cells provide several operational benefits compared with traditional grab samples and techniques such as inductively coupled plasma mass spectrometry.

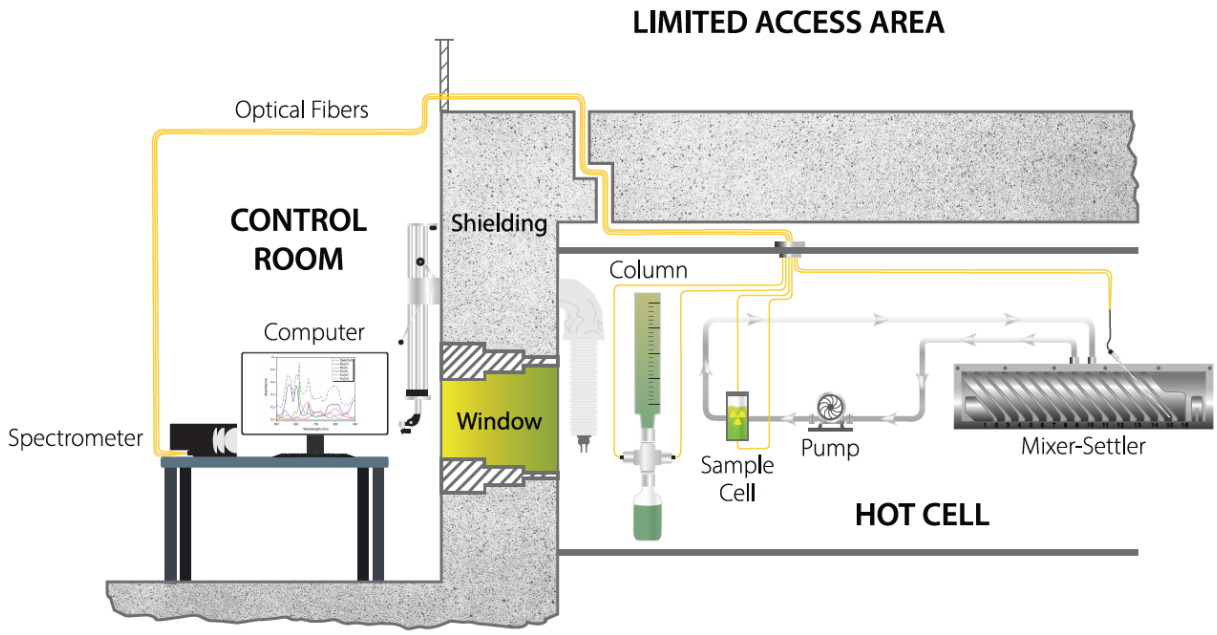

Figure 1.1. Simplified schematic showing optical measurements in a hot cell with fiber-optic cables.

Most of the development work for spectroscopy, chemometrics, and online monitoring has been focused on monitoring liquid samples to support feed adjustments and radiochemical separations. Few examples of solid-state sample characterization are available, and these methods include X-ray or neutron diffraction and scanning electron microscopy (SEM).[20, 21] These techniques are sensitive to bulk crystal structure (pXRD) and particle morphology (SEM) for the identification of crystalline materials. The characterization of the Np and Pu oxide product was identified by research staff as a moderate priority in 2021, and some development work has occurred since then to address this need.[6] Similar multivariate analysis and online monitoring techniques and concepts developed by the program for liquid processing streams could be applied to solid-state samples—particularly, Np oxide samples to support the modified direct denitration process and understanding NpO_2 properties that effect dosing for pellet fabrication.

Steps were taken to establish solid-state optical spectroscopy capabilities in FY 2023 to provide advanced characterization for the ^{238}Pu Supply Program. The development work has focused on three primary optical techniques including diffuse reflectance spectroscopy (DRS), Raman spectroscopy, and laser-induced breakdown spectroscopy (LIBS). Specifically, these techniques could be leveraged to help characterize the differences between batches of Np oxide and relate those differences back to process conditions to optimize run performance and ensure optimal product quality. Optical techniques can be leveraged to identify impurities, crystal phase, crystallite size, color, texture, and many other properties in oxide samples that could affect product quality and other parameters such as ease of incorporation into pellets and targets. This report will elaborate on these techniques, provide proof-of-concept data, and discuss plans to further develop the methods that may be pursued in more detail moving forward.

2. DIFFUSE REFLECTANCE SPECTROSCOPY

2.1 EXPERIMENTAL CONDITIONS

A range of Np oxide colors have been observed by staff performing modified direct denitration (MDD) and high-fired NpO_2 operations. These colors are poorly understood but have been correlated to qualitative Np oxide properties (e.g., dosing) and other physical properties; however, there are no definitive correlations. However, this phenomenon suggests that pursuing the quantitative assessment of Np oxide color may provide a significant benefit to the processes used to produce Np oxide and, ultimately, the ^{238}Pu Supply Program as a whole.

Oxide color could be characterized by comparisons with Munsell charts; however, this comparison is generally considered to be a qualitative test with significant user bias. Color assignments using this method are highly subjective and can vary depending on the incident lighting, the operator's color vision and perception of color (e.g., optical mixing effects and other optical illusions), and additional environmental factors or sample properties such as microstructure.[22, 23] Alternatively, collecting optical spectra for samples in the UV-Vis-NIR region enables the quantitative determination of how photons interact with the samples to produce color.[24] This technique is nondestructive and underused in the entire nuclear field but could provide unique analytical benefits.[25]

Reflectance measurements are simply the ratio of the reflected light to the incident light, and these measurements are far more quantitative than the human eye's ability to examine sample color. Light not reflected at an interface is absorbed, scattered, or transmitted. Smooth or shiny surfaces typically have high specular reflection, in which the incident light reflects into a single outgoing direction. This light is often described as *mirror-like*. Rough surfaces tend to have diffuse reflectance (DR) properties and scatter light in all directions. Many materials have both specular and DR properties.

UV-Vis-NIR DRS is a common method referring to the collection of reflected electromagnetic intensities in the region of approximately 300–1,700 nm. Peaks in DRS spectra typically correspond to electronic and/or vibrational energy levels in the sample and can be used to evaluate sample color. DRS measurements are commonly used for food processing, pharmaceutical monitoring, and environmental applications. Research and development (R&D) staff could rigorously measure the color of the Np oxide material using UV-Vis-NIR DRS (i.e., absorption) using reflection probes (see Figure 2.1) in a glove box. Data collected using this bulk, in situ approach could be compared with other advanced instrumentation at Oak Ridge National Laboratory (ORNL) (e.g., CRAIC microspectrometer). Improving the understanding of Np oxide colors will lead to an improved ability to qualify the produced Np material and retrospectively optimize MDD operational parameters when combined with additional analytical methods (e.g., pXRD) and principal component analysis (PCA). This capability could help scale up efforts and prevent faulty batches or rework.

2.2 COLD TESTS

Cold tests with lanthanide oxides, standards, and DR probes made by Ocean Insight and Hellma are promising methods (Figure 2.1). The Ocean probe was held at a 45° angle to minimize specular reflection. The probe can also be held at 90° for specular reflection, if desired. When using the Ocean probe for specular (90°) measurements, the diameter of the sample area is equal to approximately ½ the distance, d, between the probe tip and the sample. At an incidence angle of 45°, the spot becomes an oval that is $0.44d \times 0.63d$. Initial tests were also focused on evaluating the performance of each probe because the Ocean and Hellma probes cost approximately $1,200 and $12,000, respectively. The spot size of the Hellma probe can vary, but the spot size of the Ocean probe is mostly fixed at approximately 1 cm in diameter. However, the size changes slightly based on the probe distance from the sample surface and

should be kept as constant as possible. Some preprocessing methods, like standard normal variate (SNV), can be used to mitigate slight differences due to probe differences. Integrating spheres can also be used if the reflectivity of the sample changes significantly at different viewing angles. Probes are ideal for this intended application because they can make quick measurements with a relatively small spot size in a glove box.

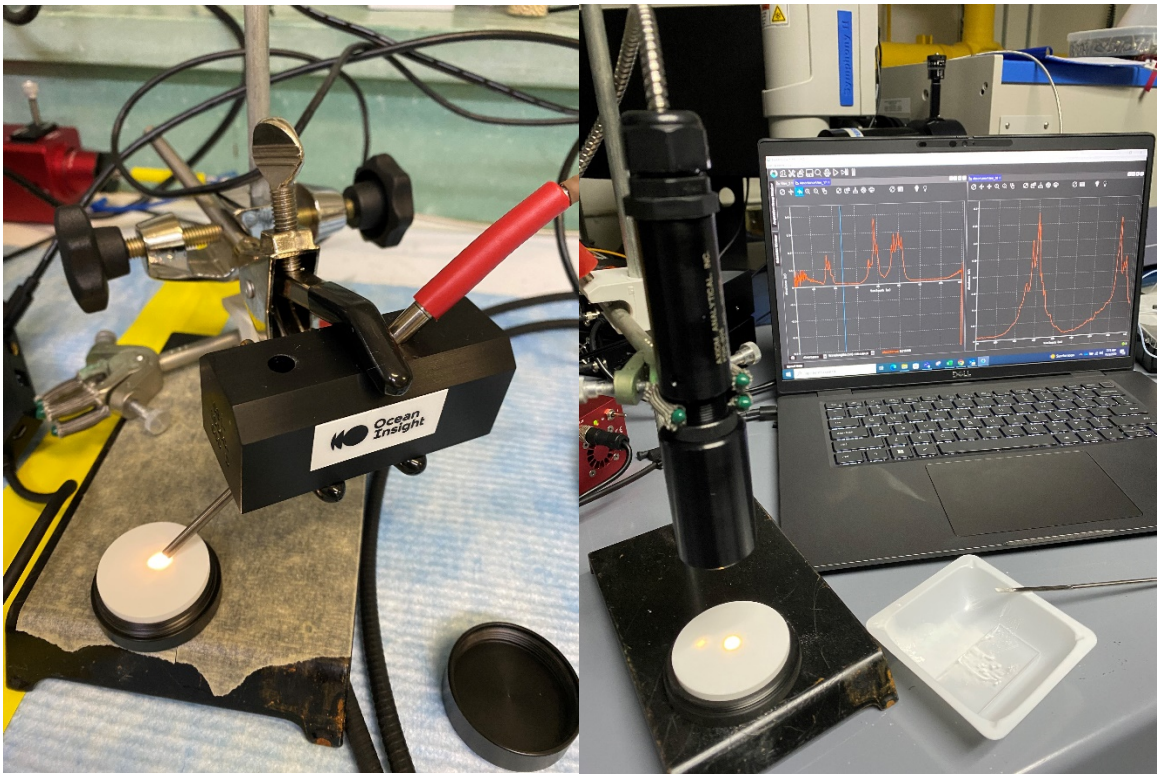

Figure 2.1. (left) Ocean Insight DR probe collecting data on a reference puck and (right) Hellma probe measuring Tm_2O_3 powder.

Several controls were evaluated prior to analyzing Np oxide, including a lanthanide oxide and reflectance standards. The reflectance spectrum (400–1,700 nm) collected with approximately 10 mg Tm_2O_3, a surrogate for Np oxide, matched literature spectra well in terms of peak position and shape.[26] Several intensity reference pucks (Labsphere) were also evaluated, and the measured intensity values were within less than approximately 5% of the specification (data not shown here). Most DR standards are matte white and use a polytetrafluoroethylene diffuser that reflects approximately 99% of the light from an approximate range of 250–1,500 nm. One option (WS-1-SL by Ocean Insight) could be good for working in the field because it can be cleaned and reused if it gets dirty or the sample is placed on the puck for the measurements.

With detector integration times of less than 1 s, users can rapidly collect Np oxide data directly in a glove box. Fiber-optic ports are already installed on glove boxes and the probe takes up minimal space. Additionally, samples could be removed from the glove box and analyzed in cold labs with advanced instrumentation.

Several options exist for preparing samples for DRS analysis. A thorough evaluation of each approach would be helpful before deciding which is best. An ideal method would likely ensure a consistent sample height relative to the reflection probe and ensure that enough material is present such that no light can be observed coming through the sample. In this study, approximately 10 mg each of two Np oxide samples

were enclosed between glass slides in a radiological fume hood (see Figure 2.2). The oxide pressed against the glass makes a flat surface that helps create a consistent working distance from the reflection probe. A bead of glue around the edges was sufficient to keep the slides together. The samples were transferred out of the radiation hood for analysis using cold instruments. If tilted, the powder can spread out to the glue edges. Too much spread could result in an insufficient spot size. The $BaSO_4$ standard, a common powder reflectance standard, was prepared the same way, and Np DRS spectra were recorded relative to this standard.

2.3 HOT SAMPLES

The qualitative colors of MDD Np_2O_5/NpO_2 and high-fired NpO_2 (~1,100 °C) are shown in Figure 2.2. The shades of brown and tan are clearly quite different; the high-fired product is lighter than the MDD product. However, additional shades of brown and other colors (e.g., orange) have also been observed (data not shown here or is unavailable). These colors can be measured quantitively and documented to begin correlating spectra features to batch conditions.

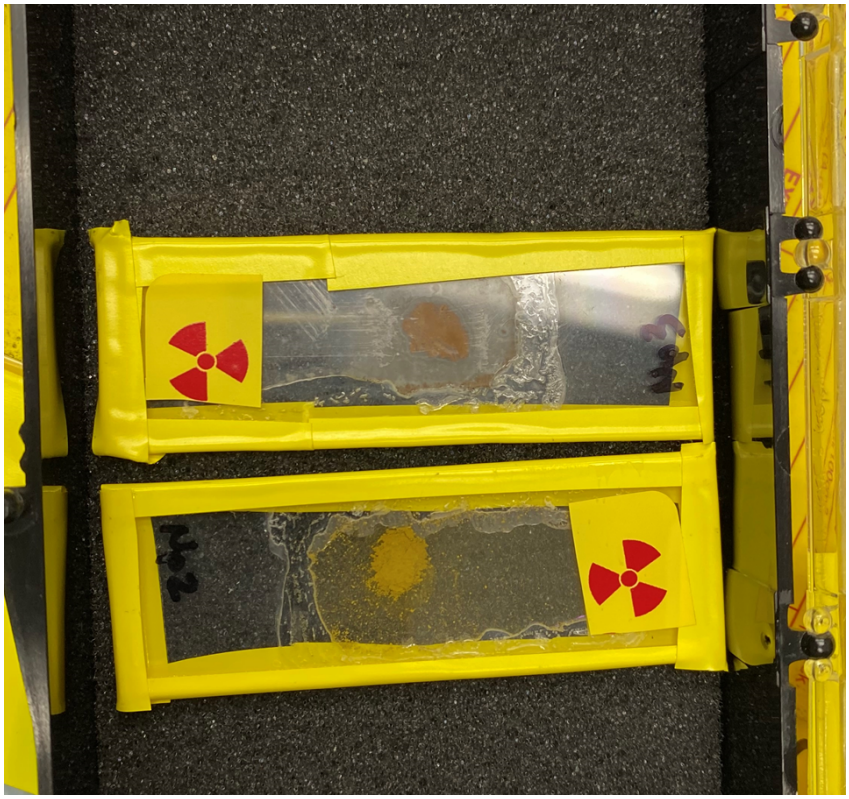

Figure 2.2. Samples prepared in glass sandwiches. Samples correspond to (top) an MDD product (Np oxide mixture) and (bottom) high-fired NpO_2.

The DRS spectrum of the MDD product is shown in Figure 2.3. Characteristic peaks near 1,050 and 1,600 nm may correspond to Np(V) electronic transitions that also appear in the aqueous Np(V) absorption spectrum at similar wavelengths. The small peaks in the NpO_2 spectrum are qualitatively similar to PuO_2 spectra (Figure 2.3).[25] No reported NpO_2 spectra appear in the literature. The fact that the color of these samples was very different, as well as their DRS spectra, is promising. The next set of experiments should compare DRS spectra from NpO_2 samples produced from different batches. Even though the long-range crystal structure quantified by pXRD may be too similar to quantify sample differences, DRS spectra could help identify variances because color is related to more than just crystal

structure. Powder X-ray diffraction is a bulk measurement technique and cannot analyze specific spots/areas but is complimentary to optical measurements.

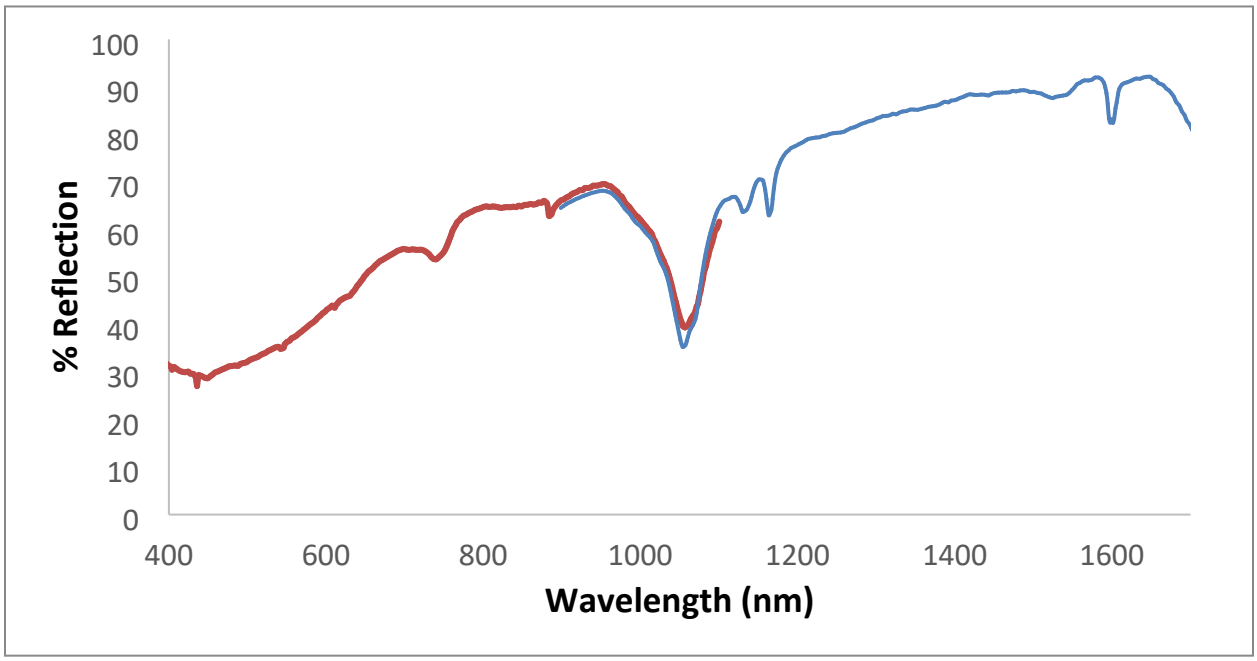

Figure 2.3. DR spectrum of the MDD product (NpO_2/Np_2O_5).

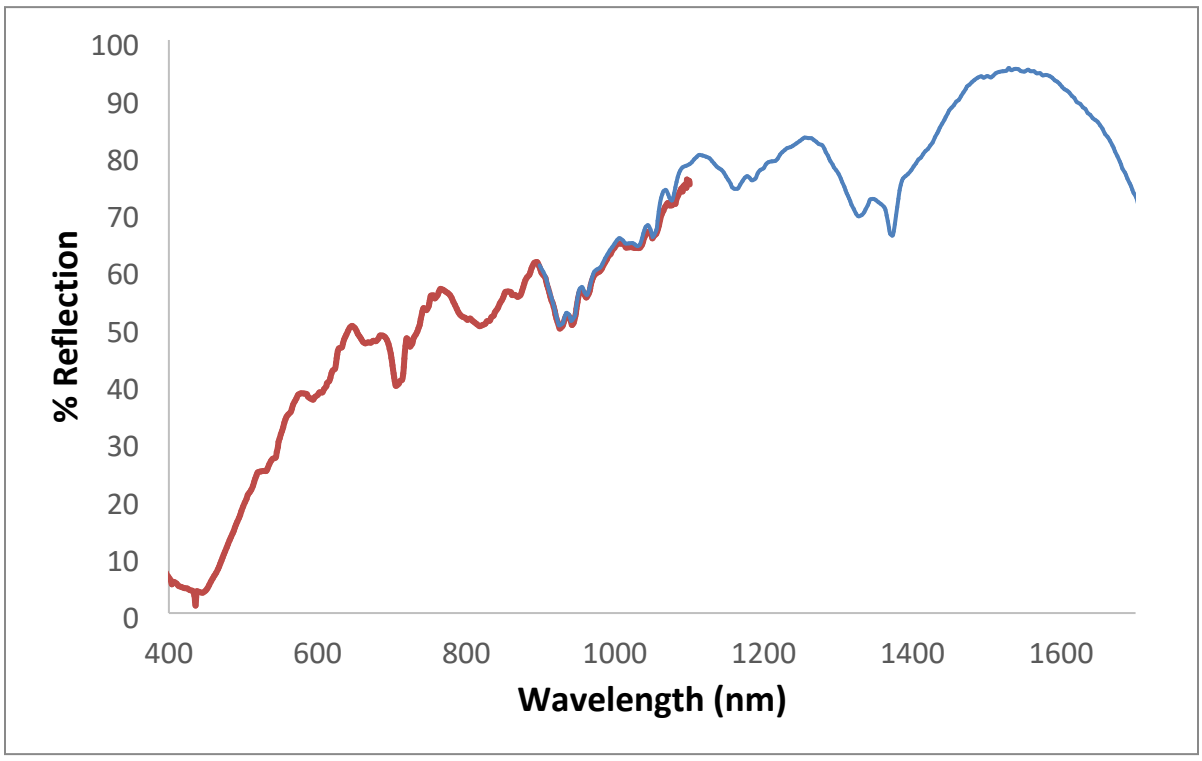

Figure 2.4. DR spectrum of the high-fired NpO_2 sample.

The exact origin of these peaks may be difficult to determine without modeling and simulation, especially because very little has been published on this topic. This research could be pursued in more fundamental

work outside of the scope needed for this project. An exact description of each peak in these spectra is not necessary because one can still leverage multivariate chemometrics for the analysis of peak characteristics for classification or even regression problems. Moving samples closer or farther away from the probe, relative to the blank sample distance, creates an appreciable baseline shift. Although keeping the distance between measurements identical is important, data processing may correct for some offset between samples. Normalizing the spectral intensity between samples may help the chemometric analysis focus more on peak wavelength positions, which may be the most indicative property.

2.4 NEXT STEPS

Data transformations, or *preprocessing*, will need to be leveraged to compensate for additive and multiplicative effects in DRS spectra. Multiplicative scatter correction was designed to deal with scattering artifacts in reflectance spectroscopy and can treat similar effects, including pathlength variations, offset shifts, and interferences. Multiplicative scatter correction uses the mean spectrum as a reference for the dataset; an assumption is that the mean is representative of each current and future spectrum collected under similar conditions. Another option for removing scatter effects is the standard normal variate transformation. Standard normal variate transformation centers and scales each individual spectrum using only data from that spectrum. Spectra are centered on zero and vary roughly between −2 and +2. After preprocessing, unsupervised classification methods can be used to reveal hidden structures in the datasets and provide a visual representation of relationships between samples and variables to better understand how samples are similar to one another.

PCA is a bilinear modeling method that takes information from the original variables and projects them onto a smaller number of latent variables called principal components (PCs). It is the primary workhorse for multivariate data analysis techniques. Each PC explains some percentage of the variation in the original dataset. This method can be used to identify sample patterns and detect gross or subtle outliers. Soft Independent Modeling of Class Analogy (SIMCA) is based on multiple PCA models for each class (e.g., MDD run) in the training set and is known as a supervised pattern recognition method. New samples are compared with each class model and assigned to a specific class (i.e., MDD run) based on similarity to the training samples.

PCA and/or SIMCA modeling techniques could be used to classify the data collected during MDD runs to identify properties of the material that indicate how well the MDD ran, if it is producing a consistent product, or if samples are outside of normal bounds. DRS spectra could easily be paired (i.e., sensor fusion) with information from other optical methods such as Raman spectroscopy and different techniques such as pXRD or SEM images to build more robust models.

3. RAMAN SPECTROSCOPY

3.1 INTRODUCTION

Raman spectroscopy investigates changes in the polarizability within a bond, giving rise to Raman scattering, which is related to individual chemical bonds within a material. Most of the laser light that contacts a sample is scattered with the same amount of energy as what it entered the system with (*elastic scattering*). A small fraction of the light interacts with the material and results in Stokes (lower energy) or Anti-Stokes (higher energy) shifts from the laser line. Stokes shifts are more intense and common in the literature.

Raman spectra contain valuable information relating to the chemical structure of a material. Band attributes (e.g., position, full width at half maximum, intensity, splitting) can change in relationship to calcination temperature, crystal lattice defects, and other perturbations. Raman spectroscopy is also a powerful tool for fast, nondestructive 2D and even 3D mapping of materials. Raman maps show the spatial distribution of spectral (i.e., chemical) information across a given sample.

Although UO_2 and PuO_2 samples have been studied in much greater detail than NpO_2, several papers in the literature describe NpO_2.[27,28] The primary Raman-active mode of the NpO_2 fluorite structure is the T_{2g} mode and can provide a fingerprint of the crystal lattice. However, the authors are not aware of any published works that characterized pure or a majority Np_2O_5 phase, which is a great opportunity for publications.[29]

3.2 INSTRUMENT DETAILS

A refurbished, lightly used LabRAM HR Evolution (Evo) Raman Microscope was purchased in FY 2023 and is shown in Figure 3.1. This instrument is essentially the same as the rebranded Horiba Odyssey system. It is a fully integrated, high-resolution, confocal Raman microscope, optimized for Vis light of 2,200 nm. The instrument is an 800 mm focal length astigmatic flat field spectrograph based on concave mirrors, which provides the highest spectral resolution on the market. It comes with 532, 633, and 785 nm continuous wave lasers, and the research team added a 405 nm laser for fluorescence using an FC/PC optical fiber mount. The instrument comes with 20× and 50× long working distance objectives and regular 10×, 50×, and 100× microscope objectives. The instrument comes with ultralow-frequency bandpass and notch filters to allow measurements typically down to 5 cm^{-1} and anti-Stokes measurements with the 532 nm laser.

The microscope has multiple scanning modes for *xy* mapping, and *z* mapping is also possible. The SWIFT Ultra-Fast feature increases the scanning speed to <5 ms per point through detector stage synchronization. The ParticleFinder software module will enable particle location, statistical analysis of particle shape/size, and automated Raman analysis. However, the particles need to be somewhat evenly dispersed for this software to function properly. The instrument also comes with a multivariate analysis package to analyze as many as millions of data points collected during mapping experiments. It can be automatically calibrated using a Si standard. The instrument can be used to analyze single particles near a single micrometer in diameter and larger samples multiple inches in diameter. The Evo also comes with a polarizer kit to help with assigning vibrational modes, and it is set up to house another charge coupled device (CCD) to optimize signal throughput. The instrument has a Class 1 enclosure and is in Lab 212, Building 7930, near REDC.

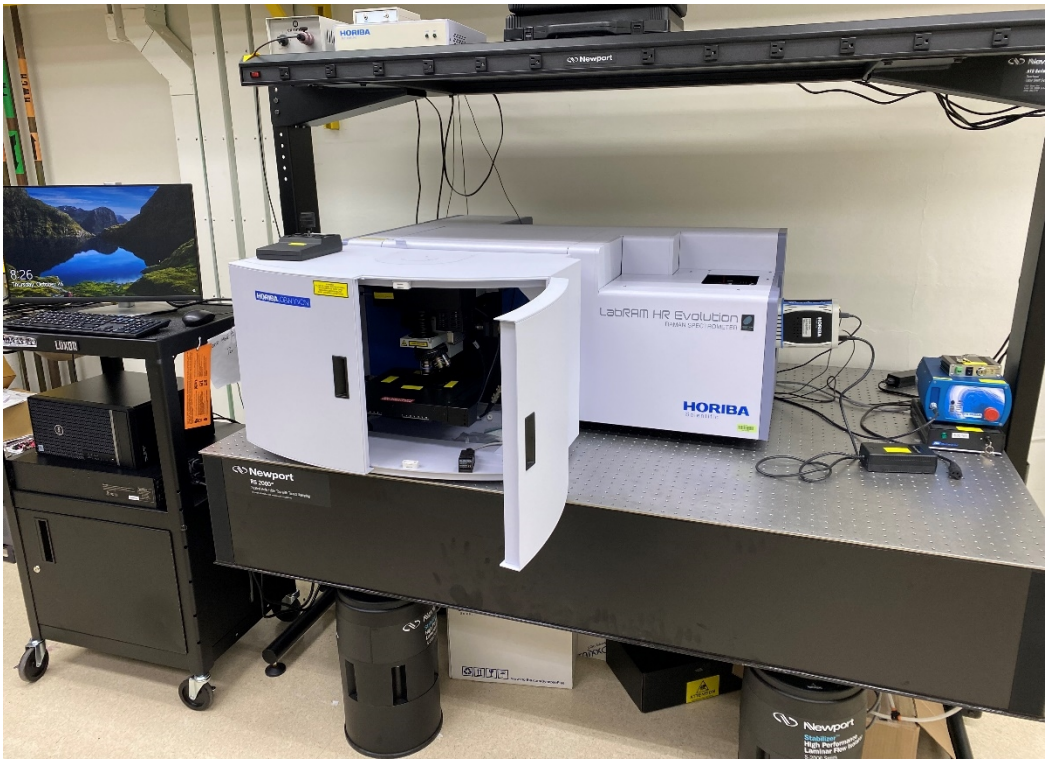

Figure 3.1. LABRAM Evolution Horiba Raman microscope.

3.3 SAMPLE HOLDER

This work developed a sample holder because commercially available off-the-shelf options are not available, and the researchers wanted to tailor it to the specific needs of this project. The holder needs to have a quartz window, seal the radiological material inside, be straightforward to use in a radiological environment while wearing gloves and other constraints, and hold the material several millimeters below the bottom of the quartz but not more than 10 mm from the top (i.e., working distance of the objective). The holder works for Raman measurements and DR measurements with the CRAIC microspectrophotometer.

The in-house-designed microscope slide fixture (MSF) is shown in Figure 3.2. Detailed assembly instruction is provided in Appendix A. The MSF can hold multiple samples, and the lid is held in place with a push pin. After preparing the sample, the edges can be wrapped with tape to provide a secondary barrier and ensure that it will not come open if accidentally dropped. It has primary and secondary gaskets to ensure the material stays inside the device.

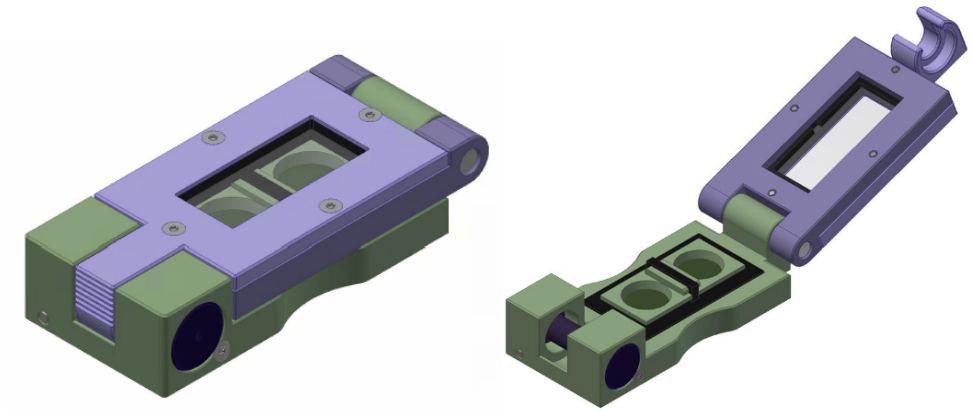

Figure 3.2. MSF (left) closed and (right) open.

Another simpler option is shown in Figure 3.3. With this approach, a 1 × 3 in. glass slide can be glued to the top to create a seal. This method likely takes hours or longer to allow the adhesive to dry but is a valid option if time is not a priority. The depth of these pockets can be adjusted easily to accommodate a taller sample (e.g., pellets) if necessary.

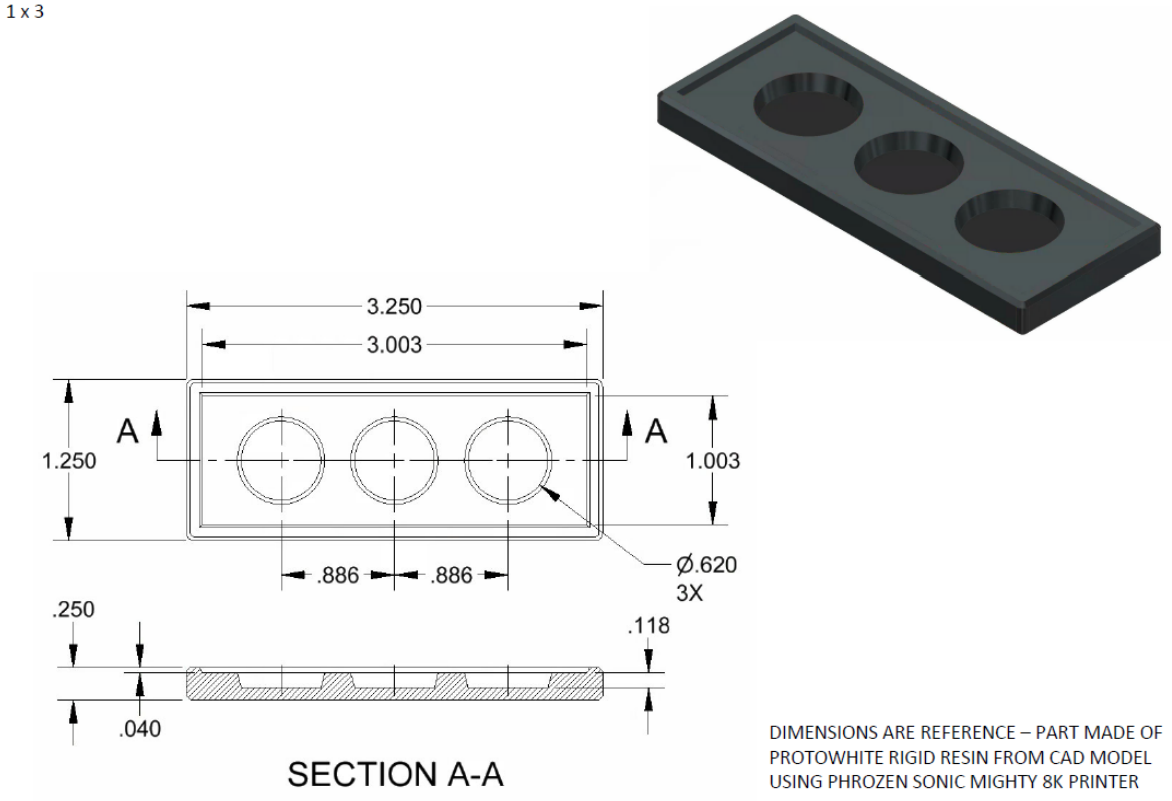

Figure 3.3. Simple 1 × 3 in. MSF option.

3.4 RAMAN SPECTRA

Two Np oxide samples were prepared for Raman analysis in the new sample holder in a radiological fume hood with RCT support. The samples were an MDD Np_2O_5/NpO_2 mixture and high-fired NpO_2 (same as that shown in Figure 2.2). Approximately 1 mg of each sample was placed in each pocket of the Raman sample holder on sticky carbon tape. The NpO_2 spectrum is shown in Figure 3.4 with important peaks noted. It took approximately 5 min to collect this spectrum. The 532 nm laser with low laser power is ideal for Np oxide measurements compared with the 633 and 785 nm options. Low power settings from 1%–2.5% were needed to ensure that the sample is not annealed by the laser heating the sample. The anti-Stokes spectrum was also collected (data not shown here) but can be used to estimate sample temperature, among other things. The Raman spectrum of NpO_2 collected on multiple spots matched the literature very well with a peak maximum near 464 cm^{-1}.[28]

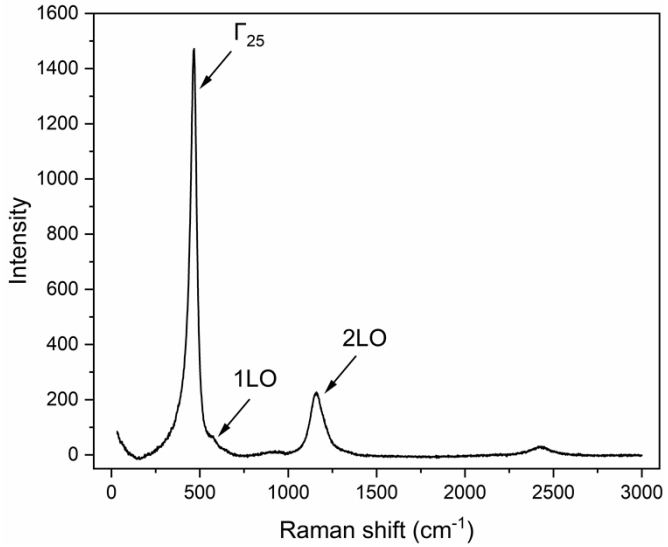

Figure 3.4. NpO_2 Raman spectrum collected with a 532 nm laser.

Raman spectra of Np_2O_5 were unique relative to NpO_2, and because of the novelty of these data, the spectra will be described in detail in a separate publication and compared to similar structures.[30] In addition to varying Np_2O_5/NpO_2 ratios, material properties, and color, small crystallites of presumably unreacted NH_4NO_3 have been noticed by staff operating the kiln. The quantity of this phase relative to the bulk is too low to be detected by pXRD (<5% of sample). For Raman analysis, the laser beam spot size with a 50× objective is approximately 1 μm in diameter and could be used to determine what these crystallites are.

3.5 NEXT STEPS

The next steps of this work will include optimizing the sample holder and Raman instrument mapping parameters. The sample holder weighs approximately 110 g. Ideally, it would weigh less than approximately 80 g so that a five-decimal place balance could be used to weigh out materials. This balance would allow more precision and accuracy when submilligram quantities need to be analyzed. Additionally, if the mapping of Np oxide cermet pellets is desired, the depth of the sample pocket can be changed. We are also working to print a holder of the MSF or something similar that can set on the stage which will make it easier for Raman measurements of similar locations after moving samples in and out.

We are also working with Horiba to evaluate a nano GPS system that can identify *xy* locations within about 1 micron. The software is compatible with all scanning electron microscopy systems and would

enable consistent analysis of specific particles between instruments.[31] We are also interested in acquiring a pin lamp that could be included in the Raman microscope objective. It emits characteristic wavelengths of light to provide a continuous reference to align spectral data collected over long periods of time (e.g., days, weeks) while mapping.

Raman maps will be acquired with varying resolution, instrument parameters, and time frames to determine the best option for rapidly characterizing MDD product and high fired NpO_2 material. There is also Np-containing material collected post MDD runs that has not been characterized in detail and Raman could be used to help provide insight into the chemical structure of this material. Mapping protocols are automated and relatively easy to set up. Once a sample is placed on the instrument and the map is set up, R&D staff can walk away while the instrument acquires the data. Then, multivariate analytical algorithms can rapidly model the spectra to identify groups and outliers and the primary sources of variation. Mapping could be useful for finding sources of chemical variation with oxide materials and characterizing cermet pellets as the quantity of NpO_2 relative to aluminum is optimized.

4. LASER-INDUCED BREAKDOWN SPECTROSCOPY

4.1 INTRODUCTION

LIBS is a versatile technique capable of measuring nearly all elements in the periodic table without physical contact and only minimal destruction. A high-energy pulsed laser is focused onto a sample surface where the energy density is great enough to ablate nanograms of the material and form a plasma. As this plasma cools, cascading electronic transitions emit photons when the ionized and excited species return to their ground states. These photons are measured to create an elemental spectrum. Because LIBS is performed using laser pulses and collected light, it is amenable to remote deployment in both hot cells and glove boxes. Between its ability to be performed rapidly and remotely as well as its sensitivity to light and heavy elements, LIBS is ideal for radiochemical processing applications. Applying LIBS for the quantification of trace elements in PuO_2 powder directly would be beneficial because the sample would not need to be digested for traditional inductively coupled plasma mass spectrometry measurements and it would avoid the time associated with separations and the analysis of challenging light elements. The greatest effect would occur if both trace elements and Pu isotope ratios would be measured. It is possible to quantify Pu isotopes by LIBS with a high-resolution instrument; however, this has not been done at ORNL.

4.2 LASER-INDUCED BREAKDOWN SPECTROSCOPY FOR IMPURITY QUANTIFICATION

LIBS was identified as a potential tool for the analysis of powdered materials (e.g., NpO_2 and PuO_2) in the ^{238}Pu Supply Program.[6] LIBS could be performed in glove boxes and hot cells to minimize the time, material, and dilutions associated with analytical measurements. LIBS could be performed by routing the laser pulse via fiber-optic cable, allowing the measurement to be performed in situ.

Traditionally, the analysis of powders via LIBS necessitates the use of pressed pellets to provide a dense, hardened sample surface to fire upon. For the ^{238}Pu Supply Program, pressing a pellet requires far more material than is desired to be used for an analytical measurement. Initially, carbon sticky tabs, or *gunshot residue* (GSR) tabs, were investigated as a substrate to adhere the powdered samples to for testing. Different powder samples containing P and S as impurities of interest and CeO_2 as a surrogate for PuO_2 were mounted onto GSR tabs and loaded into a LIBS sample chamber. Measurements were performed on an Applied Spectra J200 with a 266 nm Nd:YAG (neodymium-doped yttrium aluminum garnet) laser, a 100 µm spot size, and under a cover gas of He at 1 L min^{-1}. Several line scans were performed on each GSR tab. The before and after images of the samples are shown in Figure 4.1. Despite collecting spectra that contained the anticipated emission lines, Figure 4.1 evidences that the shockwave effect from plasma formation results in larger powder particles being blown off the GSR tabs. This effect would create an issue with radioactive materials, and thus, an alternative sampling approach was sought.

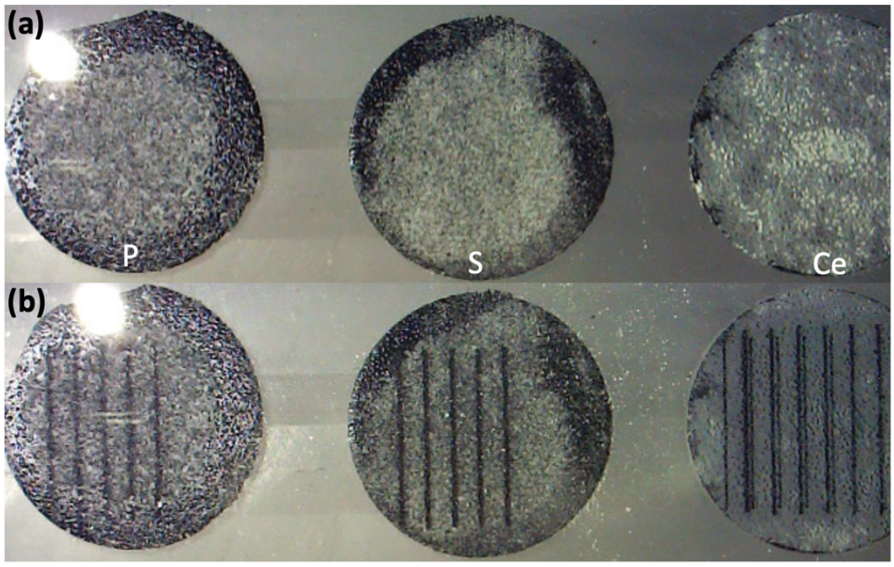

Figure 4.1. Images of GSR tabs with adhered powders containing P, S, and Ce (a) before and (b) after LIBS line scans.

The alternative sample preparation approach was to embed the powders in epoxy pellets. Epoxy is commonly used as a mounting material for larger samples, such as geological ores, because it provides a strong surface and only contributes to C and H emissions in LIBS measurements. Despite its use for larger samples, epoxy has not been investigated as an alternative for powdered samples until this point. A significant advantage of embedding powders in epoxy vs. pressed pellets is in the amount of material used. For example, a typical LIBS pellet would require approximately 300 mg of material, whereas the epoxy pellets shown subsequently only required approximately 20 mg of material, which is a 93% reduction in material costs. The initial powder epoxy pellet test sample is shown in Figure 4.2. A 2D map of the sample surface was performed using LIBS with a 50 µm spot size. The elemental maps for Ce, Na, K, and C are shown in Figure 4.2. These maps match the image of the sample epoxy pellet with the Ce, Na, and K being collocated with powder pixels and C being intense throughout (except in the case of bubble locations) because of the epoxy background.

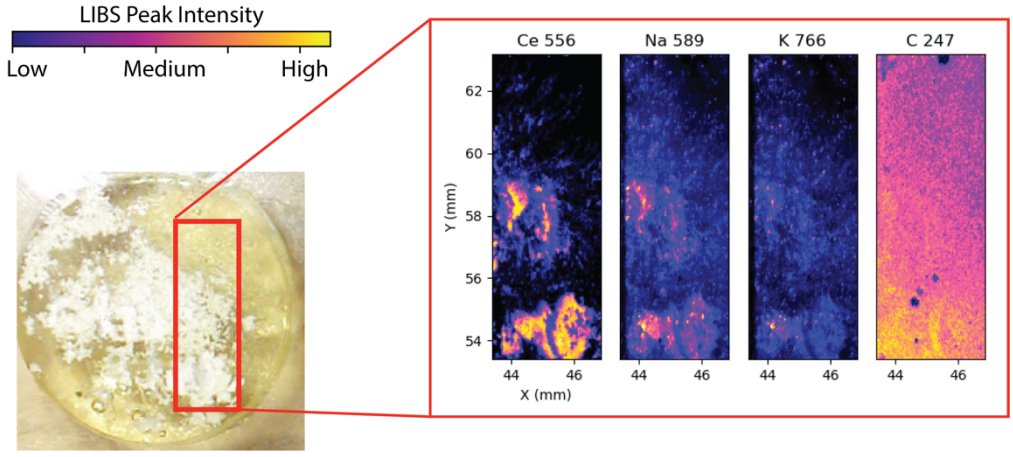

Figure 4.2. Preliminary LIBS map of CeO_2 powder embedded in epoxy resin.

Following this initial success, another pellet was made containing CeO_2 spiked with a Si impurity at 2,000 ppm. This sample was analyzed to investigate the feasibility of mapping the epoxy pellets for

impurity detection. A sample image and the LIBS maps are shown in Figure 4.3. Here, the impurity signals (Si, Na, and K) align well with the Ce pixels.

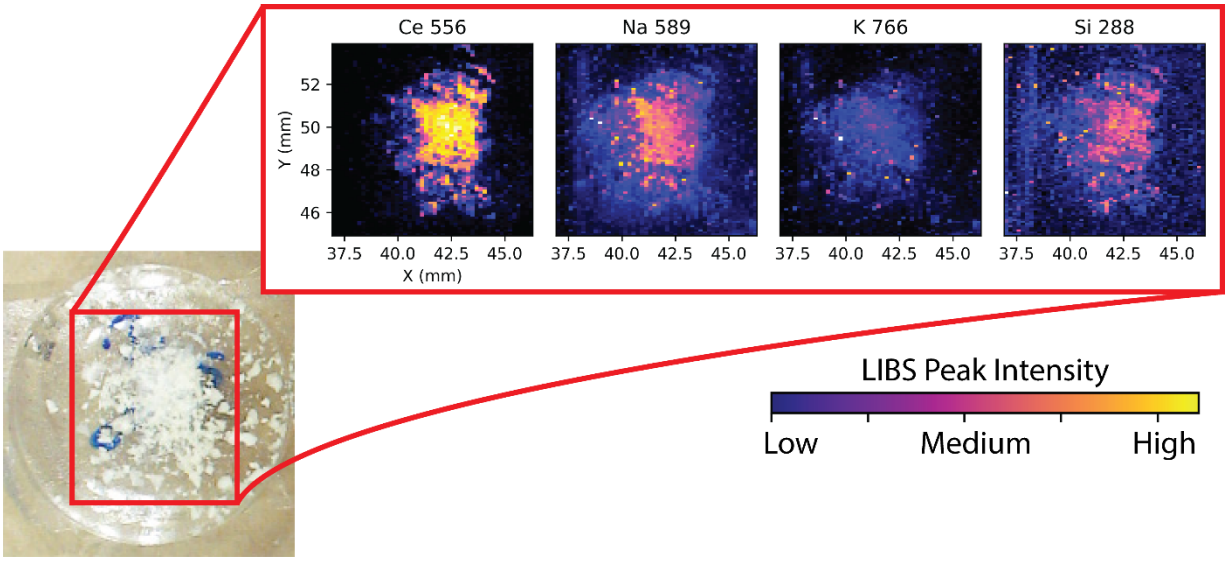

Figure 4.3. LIBS map of CeO_2 powder spiked with 2,000 ppm Si as an impurity embedded in epoxy.

By measuring a suite of these prepared epoxy pellets with varying ratios of impurities to CeO_2, calibration curves can be made to generate quantitative maps. An initial trial of these calibrations was performed, but the sample measurements identified a large level of inhomogeneity, revealing that the sample preparation procedure needed revision. With a revised sample preparation procedure to ensure accurate impurity levels in the oxide powder, a high-impact journal article on the methodology is anticipated to be produced.

4.3 LASER-INDUCED BREAKDOWN SPECTROSCOPY FOR TRANSITION PROBABILITIES

In FY 2021, LIBS was used to measure the first Np transition probabilities ever reported—a key, fundamental property needed to produce artificial LIBS spectra and perform calibration-free LIBS. Despite this success, issues were associated with the experiment that required revision prior to subsequent tests on Pu and Np/Pu mixtures. First, the sample container used to contain the radiological material was 3D printed, making it a one-time-use item because it could not be cleaned. Second, the commercial LIBS system used was not designed for shooting through optical windows. This issue resulted in back reflections, which damaged the system's optics. Lastly, the spectrometer used captured time-integrated measurements (longer exposures), which resulted in the study relying on specific assumptions about the plasma behavior.

In FY 2023, efforts were taken to resolve these experimental issues, and all the necessary changes have been made to launch the next set of experiments. A new sample chamber (Figure 4.4) was constructed using off-the-shelf parts. This sample chamber uses vacuum-compatible parts to ensure that the system is entirely sealed and not permeable throughout the duration of the testing. The top is a wedged, antireflective vacuum window to ensure that back reflections of the laser pulse cannot damage optics over the course of the measurements. The bottom uses a KF fitting so the sample may be bottom-loaded into the chamber at the boundary of a radiological hood. The chamber is then smeared by RCTs and treated as a sealed source for the remainder of the testing. In tandem with this sample chamber design, a new LIBS measurement system has been constructed in Building 7930, Lab 212. This LIBS configuration fires a

1,064 nm laser directly down into the sample chamber, and the light is collected in the same direction. A dichroic mirror is positioned above the sample chamber at a 45°. This dichroic mirror allows light above 1,000 nm to pass through it and light below 1,000 nm to be reflected, so it reflects the plasma emissions into an optical fiber for a spectral measurement without the concern of reflecting the 1,064 nm laser itself. The use of this LIBS system also provides the flexibility to modify the configuration more readily if needed.

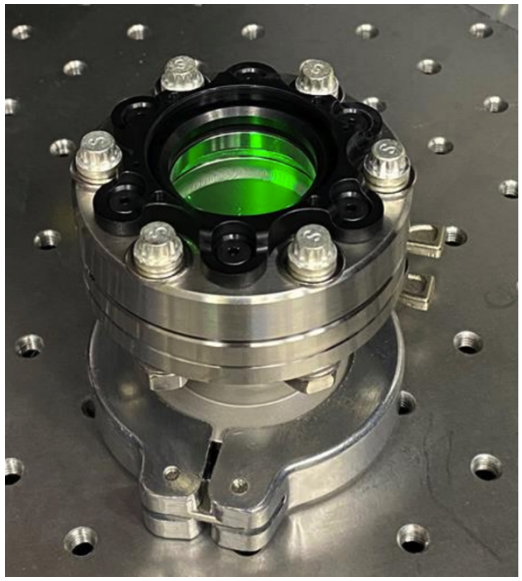

Figure 4.4. Revised LIBS sample chamber for testing radioactive samples.

Lastly, a new spectrometer (Andor Mechelle 5000, Figure 4.5) was procured. It uses an echelle grating to cover the entire UV-Vis-NIR wavelength range used for LIBS (300–1,000 nm) in a single acquisition. The detector is an intensified charge coupled device (ICCD), which provides greater sensitivity than standard nonintensified CCDs, but more importantly can be nanosecond gated. This nanosecond gating allows the LIBS plasma to be observed for very finite periods of time. These time-resolved measurements circumvent the need for the plasma assumptions used in the previous studies and mitigate errors from later in the plasma lifetime.

Figure 4.5. Andor Mechelle 5000 spectrometer with iStar ICCD camera purchased for future actinide LIBS measurements.

4.4 NEXT STEPS

Learning from previous studies, ORNL is now able to test several actinide systems to report new transition probabilities, build spectral libraries of key species, and publish several high-impact journal articles. The researchers are also ready to continue impurity analysis in oxide materials to optimize sample preparation and acquisition parameters as well as identify the limits of detection for important species. The spectral libraries built in these experiments will be essential to the growth of applied LIBS for the ^{238}Pu Supply Program and other LIBS radionuclide measurements (e.g., safeguards).

5. OUTCOMES AND FUTURE WORK

Significant progress was made to establish optical techniques for characterizing solid-state materials (e.g., oxides, pellets) for the ^{238}Pu Supply Program. DR and Raman spectroscopy appear to be useful for analyzing Np/Pu oxide samples. The methods are nondestructive and can provide timely feedback potentially in line with various processes in glove box operations are require small sample quantities. DRS is most amenable to simple glove box–deployable measurements in the near term. It does not require special approval and requires a small probe in a glove box. The light sources and fiber-optic cables currently being used for spectrophotometry are compatible with DR measurements. The new high-resolution Raman spectrometer can be leveraged for rapid chemical mapping of oxides and pellets. LIBS may be useful for quantifying trace elements and Pu isotopes, but significant development work and US Department of Energy approvals are required prior to implementation. Spectral data from optical methods can provide important and complementary data that should be combined with other techniques (e.g., pXRD, SEM) to support solid-state sample characterization for the ^{238}Pu Supply Program.

6. REFERENCES

[1] Sadergaski, L. R., S. E. Gilson, D. E. Benker, L. H. Delmau, and A. J. Parkison. 2023. *Spectrophotometric Analysis of P6PX-1 for the Pu-238 Supply Program*. ORNL/TM-2023/3197. Oak Ridge, Tennessee: Oak Ridge National Laboratory.

[2] Sadergaski, L. R.; D. R. Giuliano, and T. D. Hylton. 2022. *Hot Cell Spectrophotometry Equipment to Support the Plutonium-238 Supply Program*. ORNL/TM-2022/2540. Oak Ridge, Tennessee: Oak Ridge National Laboratory.

[3] Sadergaski, L. R., and T. Hager. 2022. *Measuring Hydroxylammonium, Nitrate, and Nitrite Concentration with Raman spectroscopy for the ^{238}Pu Supply Program*. ORNL/TM-2021/2122. Oak Ridge, Tennessee: Oak Ridge National Laboratory.

[4] Sadergaski, L. R., et al. 2022. *Spectrophotometric Analysis of N8MX-1 Neptunium Monoamide Extraction Run for the ^{238}Pu Supply Program*. ORNL/TM-2022/2508. Oak Ridge, Tennessee: Oak Ridge National Laboratory.

[5] Sadergaski, L. R., K. K. Patton, G. K. Toney, D. W. DePaoli, and L. H. Delmau. 2021. *Measuring Neptunium Concentration Using Optical Spectrometry for the Plutonium-238 Supply Program*. ORNL/TM-2021/2072. Oak Ridge, Tennessee: Oak Ridge National Laboratory.

[6] Sadergaski, L. R., K. G. Myhre, L. H. Delmau, D. W. DePaoli, and R. W. Wham. 2021. *Status of Spectroscopy and Online Monitoring for the Plutonium-238 Supply Program*. ORNL/TM-2021/1922. Oak Ridge, Tennessee: Oak Ridge National Laboratory.

[7] Sadergaski, L. R., S. S. Schwengels, L. H. Delmau, D. E. Benker, D. W. DePaoli, and R. M. Wham. 2021. "Online Monitoring of Radiochemical Processing Streams for the Plutonium-238 Supply Program." In *Nuclear and Emerging Technologies for Space*. Washington, DC: National Aeronautics and Space Administration.

[8] Sadergaski, L. R., D. E. Benker, D. W. DePaoli, R. M. Wham, and L. H. Delmau. 2021. *Spectrophotometric Analysis of P5PX-1 to Support the Pu-238 Supply Program.* ORNL/TM-2021/2317. Oak Ridge, Tennessee: Oak Ridge National Laboratory.

[9] Sadergaski, L. R., S. S. Schwengels, L. H. Delmau, and D. W. DePaoli. 2021. *Monitoring Radiochemical Processing Streams for the Pu-238 Supply Program with Process Pulse II*. ORNL/TM-2021/13. Oak Ridge, Tennessee: Oak Ridge National Laboratory

[10] Sadergaski, L. R., K. G. Myhre, L. H. Delmau, D. E. Benker, D. W. DePaoli, and R. M. Wham. 2020. "Spectroscopic and Multivariate Analysis Development in Support of the Plutonium-238 Supply Program." In *Nuclear and Emerging Technologies for Space*. Washington, DC: National Aeronautics and Space Administration.

[11] Sadergaski, L. R., H. B. Andrews, S. B. Gilson, and A. Parkison. 2023. "Quantifying Neptunium Oxidation States in Nitric Acid through Spectroelectrochemistry and Chemometrics." *Frontiers in Nuclear Engineering* (Nuclear Materials Section) 2, 1323372. DOI: 10.3389/fnuen.2023.1323372.

[12] Andrews, H. B., and L. R. Sadergaski. 2023. "Hierarchical Modeling to Enhance Spectrophotometry Measurements—Overcoming Dynamic Range Limitations for Remote Monitoring of Neptunium." *Chemosensors* 11, 274. DOI: 10.3390/chemosensors11050274.

[13] Andrews, H. B., and L. R. Sadergaski. 2023. "Leveraging Visible and Near-Infrared Spectroelectrochemistry to Calibrate a Robust Model for Vanadium(IV/V) in Varying Nitric Acid and Temperatures Levels." *Talanta* 259, 124554. DOI: 10.1016/j.talanta.2023/124554.

[14] Sadergaski, L. R., and K. Morgan. 2022. “Applying Two-Dimensional Correlation Spectroscopy and Principal Component Analysis to Understand how Temperature Affects the Neptunium(V) Absorption Spectrum.” *Chemosensors* 10, no. 11, 475. DOI: 10.3390/chemosensors10110475.

[15] Sadergaski, L. R., K. G. Myhre, and L. H. Delmau. 2022. “Multivariate Chemometric Methods and Vis-NIR Spectrophotometry for Monitoring Plutonium-238 Anion Exchange Column Effluent in a Radiochemical Hot Cell.” *Talanta Open* 5, 100120. DOI: 10.1016/j.talo.2022.100120.

[16] Andrews, H. B., L. R. Sadergaski, and K. G. Myhre. 2022. “Neptunium Transition Probabilities Estimated through Laser Induced Breakdown Spectroscopy (LIBS) Measurements.” *Journal of Analytical Atomic Spectrometry* 37, no. 4, 768–774. DOI: 10.1039/D1JA00423A.

[17] Sadergaski, L. R., T. J. Hager, and H. B. Andrews. 2022. “Design of Experiments, Chemometrics, and Raman Spectroscopy for the Quantification of Hydroxylammonium, Nitrate, and Nitric Acid.” *ACS Omega* 8, 7287–7286. DOI: 10.1021/acsomega.1c07111.

[18] Sadergaski, L. R., G. K. Toney, L. H. Delmau, and K. G. Myhre. 2021. “Chemometrics and Experimental Design for the Quantification of Nitrate Salts in Nitric Acid: Near-Infrared Spectroscopy Absorption Analysis.” *Applied Spectroscopy* 75, no. 9, 1155–1167. DOI: 10.1177/0003702820987281.

[19] Sadergaski, L. R., D. W. DePaoli, and K. G. Myhre. 2020. “Monitoring the Caustic Dissolution of Aluminum Alloy in a Radiochemical Hot Cell Using Raman Spectroscopy.” *Applied Spectroscopy* 74, no. 10, 1252–1262. DOI: 10.1177/0003702820933616.

[20] Frontzek, M. D., L. R. Sadergaski, S. K. Cary, and B. K. Rai. 2023. “Search for Octupolar Order in NpO_2 by Neutron Diffraction.” *Journal of Solid State Chemistry* 321, 123875. DOI: 10.1016/j.jssc.2023.123875.

[21] Peruski, K. M., C. J. Parker, ad S. K. Cary. 2023.“Analysis of Neptunium Oxides Produced Through Modified Direct Denitration.” *Journal of Nuclear Materials* 587, 154704. DOI: 10.1016/j.jnucmat.2023.154704.

[22] Nickerson, D. 1940. “History of the Munsell Color System and Its Scientific Application.” *Journal of the Optical Society of America* 30, 575–586.

[23] R. Benz, R. M. Douglass, F. H. Kruse, and R. A. Penneman. 1963. “Preparation and Properties of Several Ammonium Uranium(IV) and Ammonium Plutonium(IV) Fluorides.” *Inorganic Chemistry* 2, 799–803. DOI: 10.1021/ic50008a033.

[24] Villa-Aleman, E., J. H. Christian, J. R. Darvin, B. J. Foley, D. D. Dick, B. Fallin, and K. A. S. Fessler. 2023. “Diffuse Reflectance Spectroscopy and Principal Component Analysis to Retrospectively Determine Production History of Plutonium Dioxide.” *Applied Spectroscopy* 77, 449–456. DOI: 10.1177/00037028221145724.

[25] Hobart, D. E. 2011. “Diffuse Reflectance Spectroscopy of Plutonium Solids.” *Actinide Research Quarterly* 2.

[26] Runowski, M.; Stopikaowska, N.; Lis, S. 2020. “UV-Vis-NIR absorption spectra of lanthanide oxides and fluorides.” *Dalton Trans.* 49, 2129-2137. DOI: 10.1039/C9DT04921E.

[27] Villa-Aleman, E.; Houk, A. L.; Shehee, T. C.; Bridges, N. J. 2021. “Raman Signature from Age-Dating PuO_2 Since Last Calcination.” *Journal of Nuclear Materials* 551, 152969. DOI: 10.1016/j.jnucmat.2021.152969.

[28] Naji, M., N. Magnani, J.-Y. Colle, O. Beneš, S. Stohr, R. Caciuffo, R. J. M. Konings, and D. Manara. 2016. “Raman Scattering from Decoupled Phonon and Electron States in NpO_2.” *Journal of Physical Chemistry C* 120, no. 9, 4799–4805. DOI: 10.1021/acs.jpcc.5b12068.

[29] Sarsfield, M. J.; Taylor, R. J.; Puxley, C.; Steele, H. M. 2012. “Raman spectroscopy of plutonium dioxide and related materials.” *J. Nucl. Mater.* 427, 333-342.

[30] Smirnov, M. B., E. M. Roginskii, K. S. Smirnov, R. Baddour-Hadjean, and J.-P. 2018. “Pereira-Ramos. Unraveling the Structure–Raman Spectra Relationships in V_2O_5 Polymorphs via a Comprehensive Experimental and DFT Study. *Inorganic Chemistry*, 57, 9190–9204. DOI: 10.1021/acs.inorgchem.8b01212.

[31] Acher, O.; Nguyen, T-L.; Podzorov, A.; Leroy, M.; Carles, P-A.; Legendre, S. 2021. “An efficient solution for correlative microscopy and co-localized observations based on multiscale multimodal machine-readable nanoGPS tags.” *Meas. Sci. Technol.,* 32, 045402. DOI: 10.1088/1361-6501/abce39.

APPENDIX A. SUMMARY OF MICROSCOPE SLIDE FIXTURE ASSEMBLY INSTRUCTIONS

APPENDIX A. SUMMARY OF MICROSCOPE SLIDE FIXTURE ASSEMBLY INSTRUCTIONS

Microscope Slide Fixture (MSF) Assembly Instructions – PARTS LIST
20231122

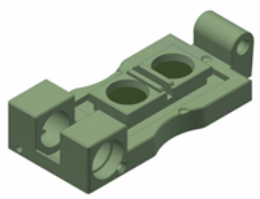

MSF FLIPPER 2B6 BOTTOM
PRINTED IN PROTOWHITE RIGID RESIN
USING PHROZEN SONIC MIGHTY 8K
QTY: 1

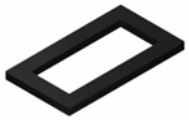

MSF FLIPPER GASKET
CLOSED-CELL POLYETHYLENE FOAM
CUT USING 1:1 DXF
QTY: 2

MSF FLIPPER 2 MIDDLE GASKET
CLOSED-CELL POLYETHYLENE FOAM
CUT USING 1:1 DXF
QTY: 1

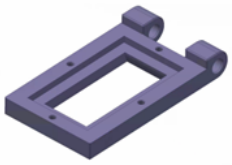

MSF FLIPPER 2B4 TOP A
PRINTED IN PROTOWHITE RIGID RESIN
USING PHROZEN SONIC MIGHTY 8K
QTY: 1

MSF FLIPPER BOTTOM GASKET
CLOSED-CELL POLYETHYLENE FOAM
CUT USING 1:1 DXF
QTY: 1

MICROSCOPE SLIDE
QTY: 1

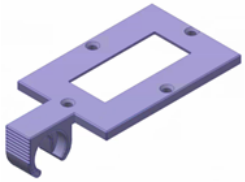

MSF FLIPPER 2B6 TOP B
PRINTED IN PROTOWHITE RIGID RESIN
USING PHROZEN SONIC MIGHTY 8K
QTY: 1

DOWEL PIN, ¼ DIA, 1-3/4 LG, 18-8 SST
MCMASTER-CARR P/N 90145A548
QTY: 1

MAGNET, 1/8 DIA, 3/8 LG, N52
MCMASTER-CARR P/N 5862K122
QTY: 2

MSF FLIPPER 2B6 PIN A
PRINTED IN PROTOWHITE RIGID RESIN
USING PHROZEN SONIC MIGHTY 8K
QTY: 1
(4 PRINT FILES – CHOOSE ONE THAT FITS BEST)

MSF FLIPPER 2B5 PIN B
PRINTED IN PROTOWHITE RIGID RESIN
USING PHROZEN SONIC MIGHTY 8K
QTY: 1

PLASTITE SCREW, FLAT HEAD, #4-20, 1/2 LG, 18-8 SST
MCMASTER-CARR P/N 95893A615
QTY: 5

DOWEL PIN, 1/8 DIA, 7/8 LG, 18-8 SST
MCMASTER-CARR P/N 90145A474
QTY: 1

2

Microscope Slide Fixture (MSF) Assembly Instructions – REAMING THE FLIPPER 2B6 BOTTOM AFTER PRINTING
20231122

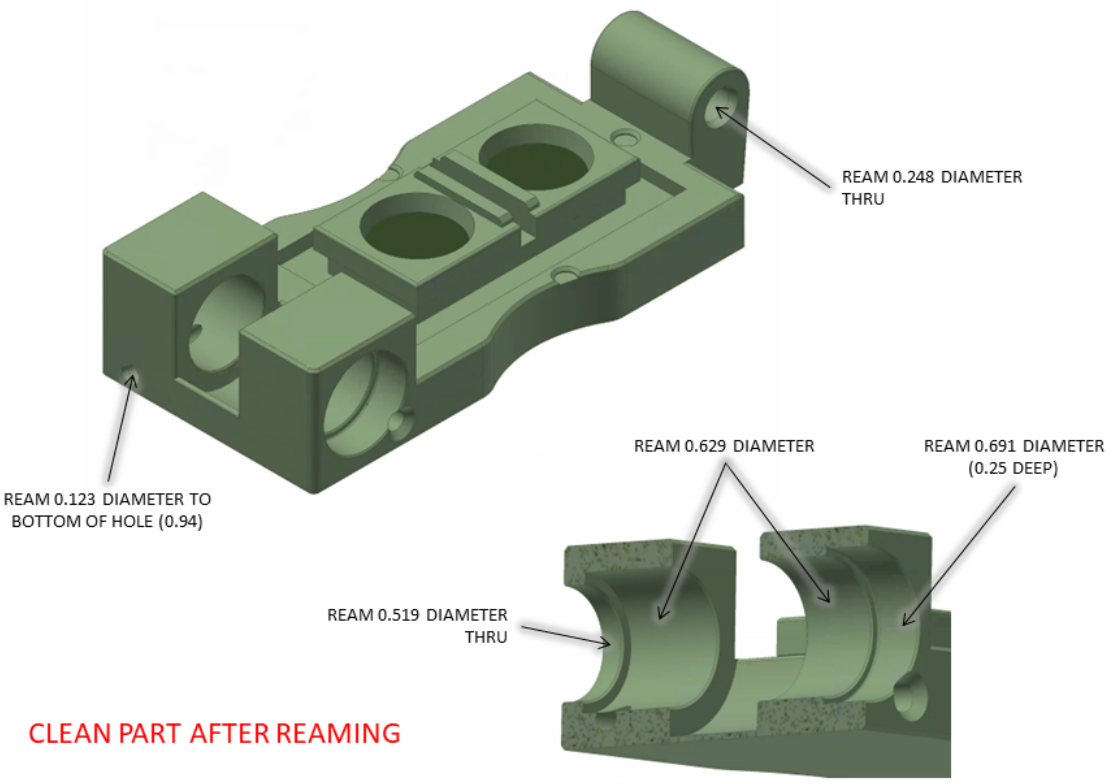

CLEAN PART AFTER REAMING

3

Microscope Slide Fixture (MSF) Assembly Instructions – FLIPPER 2B6 BOTTOM ASSEMBLY
20231122

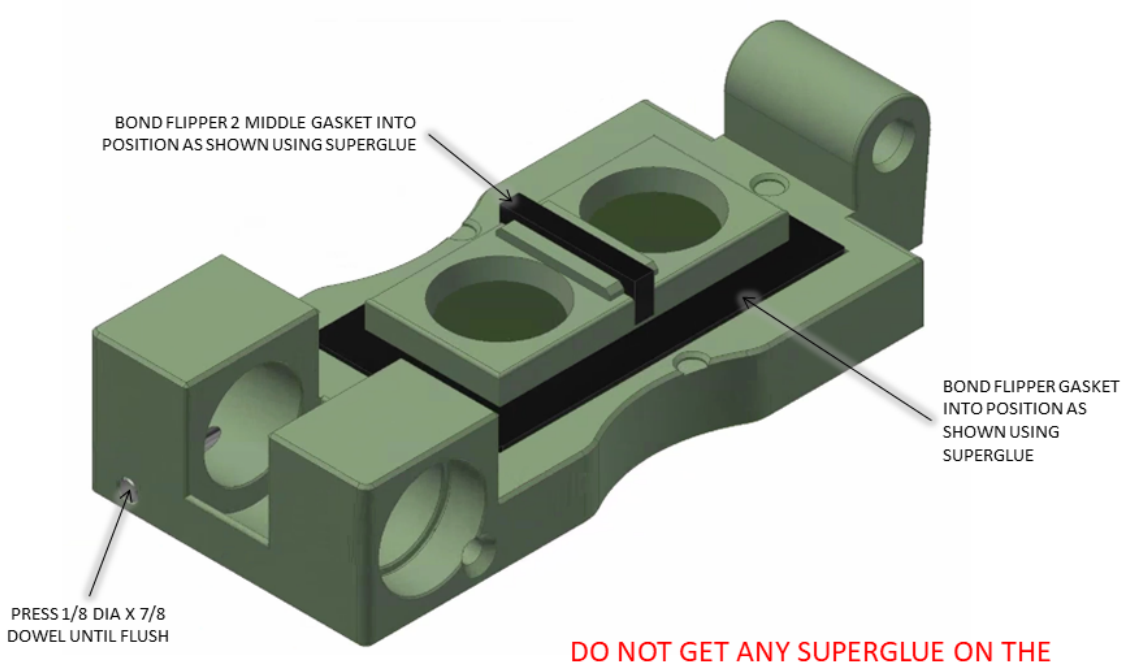

DO NOT GET ANY SUPERGLUE ON THE EXPOSED SURFACES OF THE FOAM

4

Microscope Slide Fixture (MSF) Assembly Instructions – CHOOSING THE BEST FIT OF THE FLIPPER 2B6 PIN A AFTER PRINTING
20231122

DEPENDING ON HOW ACCURATELY THE .123 DIAMETER HOLE IS REAMED IN THE FLIPPER BOTTOM, ONE OF THE FOUR PRINTED PIN As WILL FIT INTO THE BOTTOM BETTER THAN THE OTHERS. THE FIT SHOULD ALLOW EASY MOVEMENT INSIDE THE BOTTOM WITHOUT HAVING MORE CLEARANCE THAN NECESSARY. AFTER CHOOSING THE BEST FITTING PIN, SET THE OTHERS ASIDE.

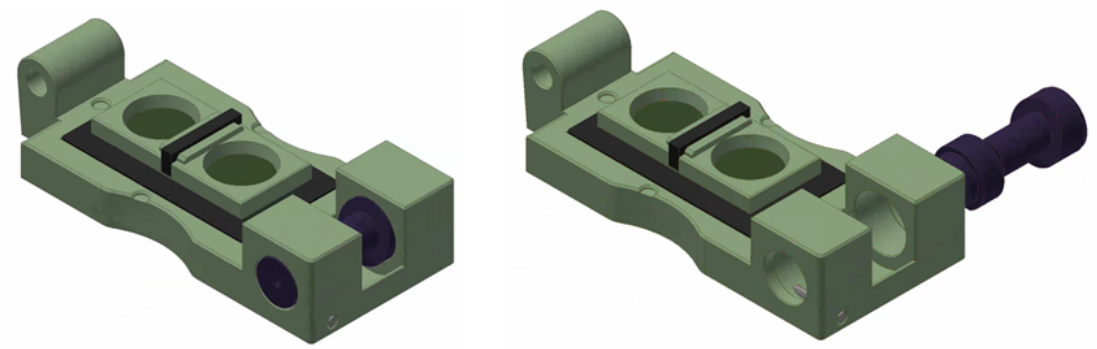

FLIPPER 2B6 PIN A MUST BE ABLE TO SLIDE EASILY OVER THE DOWEL PIN WITHOUT ROTATING.

5

Microscope Slide Fixture (MSF) Assembly Instructions – MODIFYING THE PINS AFTER PRINTING
20231122

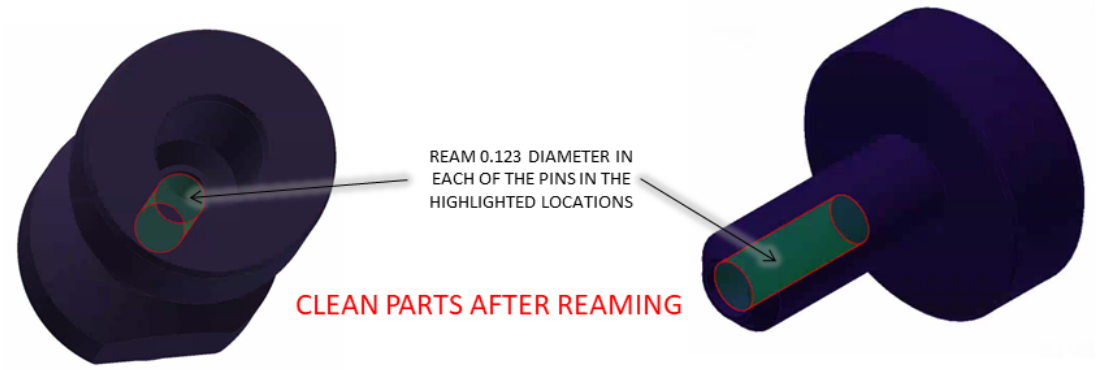

AFTER REAMING EACH PIN, PRESS A MAGNET INTO EACH AS SHOWN – BE CAREFUL TO ORIENT THE MAGNETS SO THAT WHEN PIN B IS INSERTED INTO PIN A, THE MAGNETS ARE REPULSED.

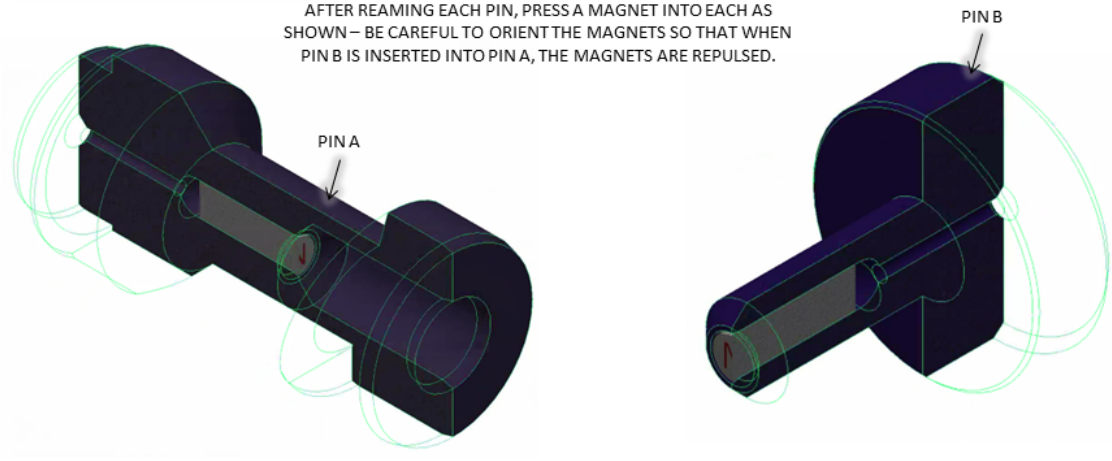

6

Microscope Slide Fixture (MSF) Assembly Instructions – REAMING THE TOP PARTS
20231122

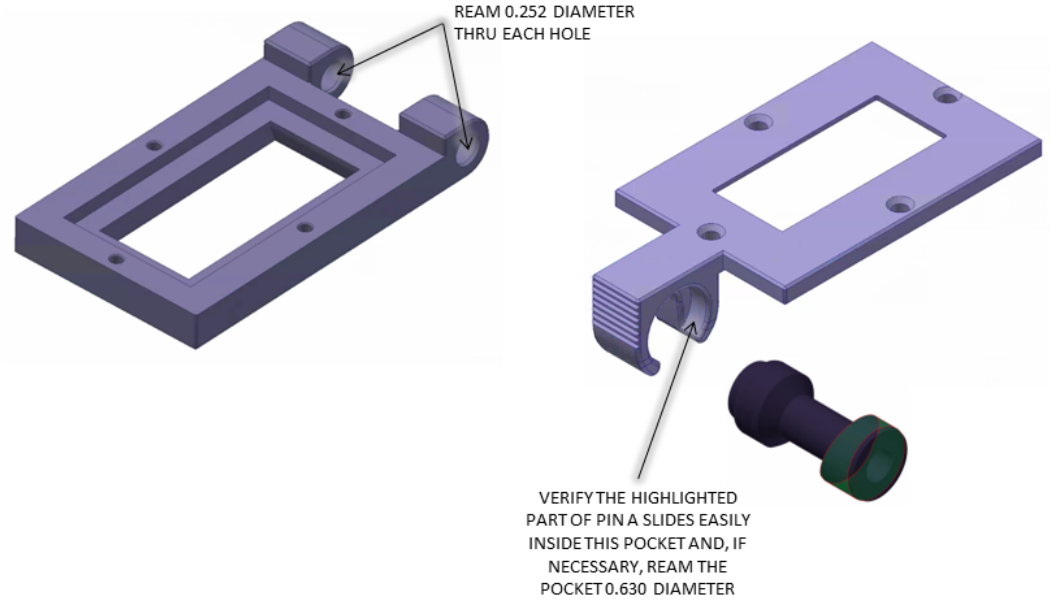

CLEAN PARTS AFTER REAMING

Microscope Slide Fixture (MSF) Assembly Instructions – FLIPPER 2B6 TOP ASSEMBLY
20231122

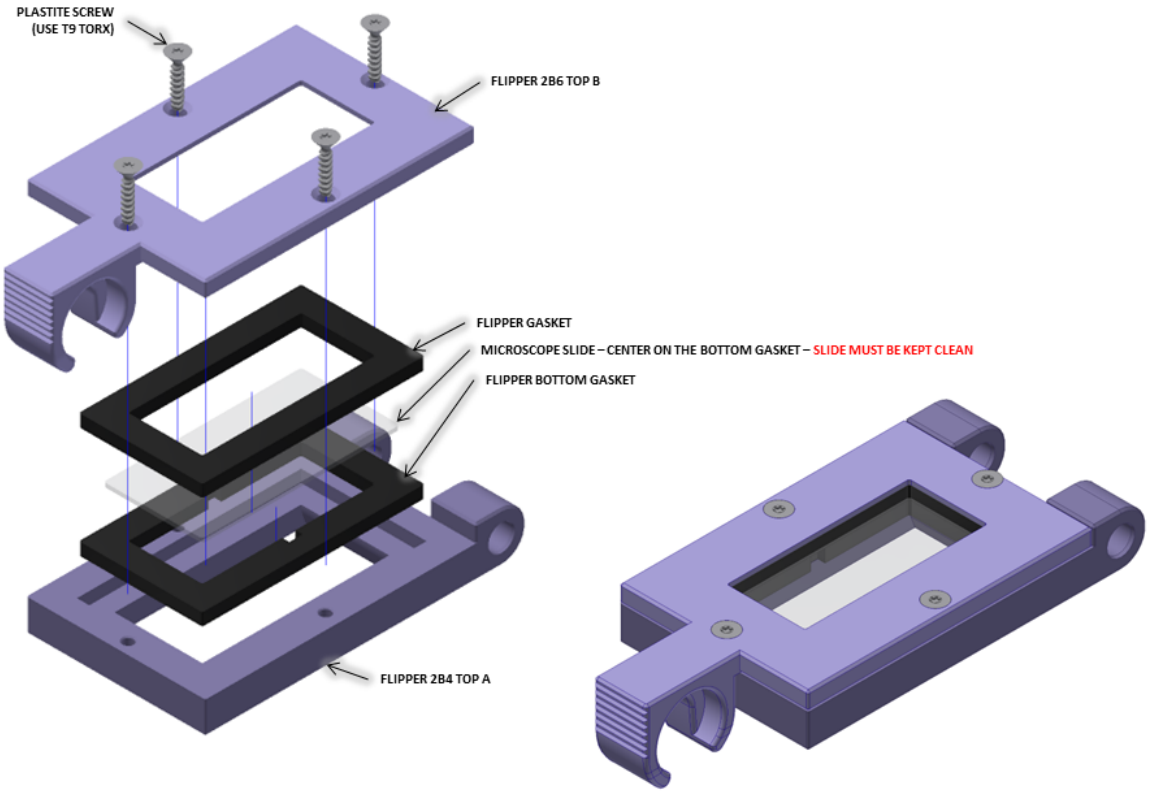

8

Microscope Slide Fixture (MSF) Assembly Instructions – ASSEMBLE PINS TO THE BOTTOM ASSEMBLY
20231122

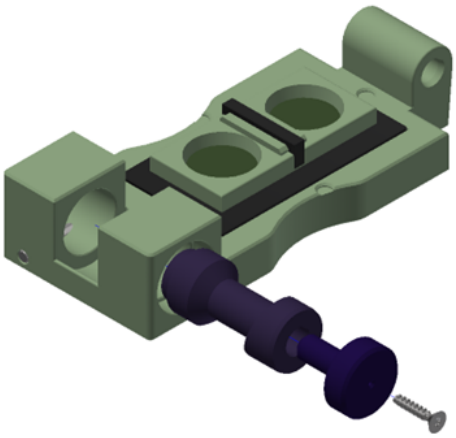

ONCE ASSEMBLED, PIN A SHOULD MOVE EASILY TOWARDS PIN B WHEN PUSHED AND SHOULD READILY RETURN TO ITS RESTING POSITION WHEN RELEASED. IF NECESSARY, APPLY A THIN LAYER OF APPROVED LUBRICANT TO THE PIN TO FACILITATE THE REQUIRED ACTION.

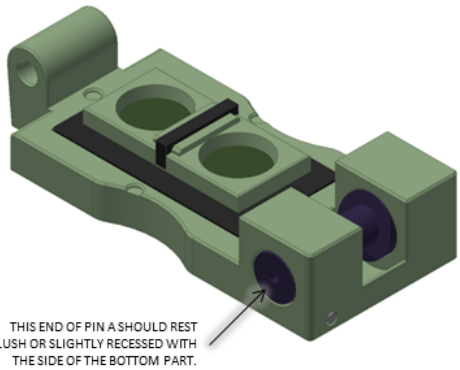

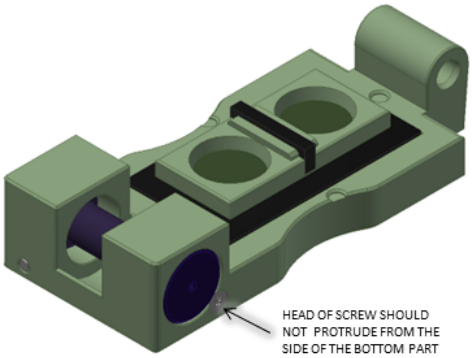

9

Microscope Slide Fixture (MSF) Assembly Instructions – ASSEMBLE THE FLIPPER 2B6 TOP ASSEMBLY TO THE REMAINING COMPONENTS
20231122

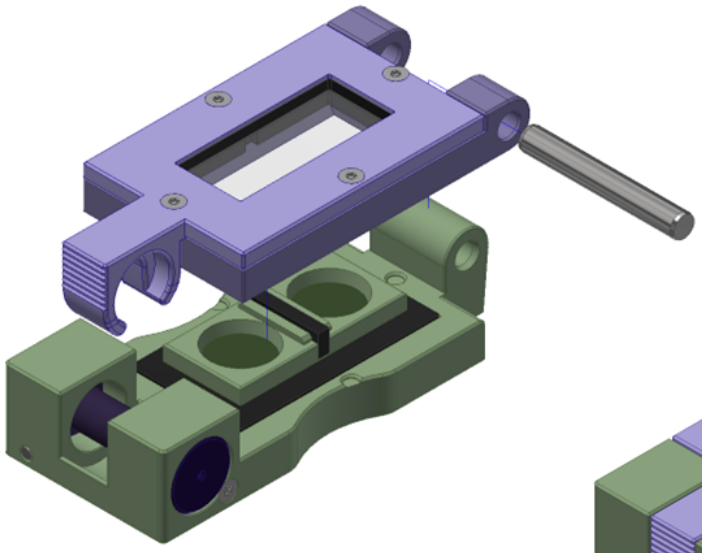

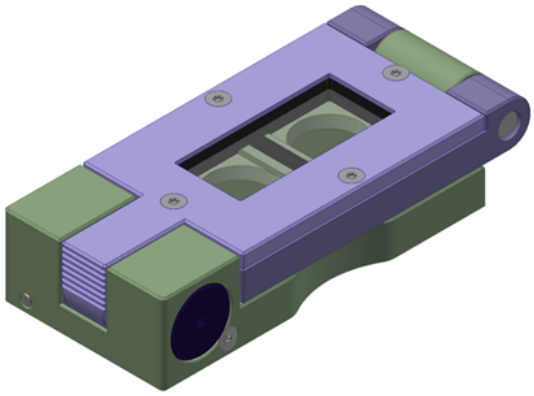

POSITION THE TOP ASSEMBLY ONTO THE BOTTOM ASSEMBLY AND PRESS IN THE DOWEL PIN. ONCE ASSEMBLED, THE TOP ASSEMBLY SHOULD PIVOT EASILY ON THE BOTTOM ASSEMBLY. THE LATCH ON PIN A IS RELEASED BY PRESSING PIN A TOWARD PIN B. VERIFY THAT LATCHING AND UNLATCHING IS WORKING PROPERLY. THE TOP ASSEMBLY SHOULD NOT UNLATCH UNLESS PIN A IS PRESSED.

10

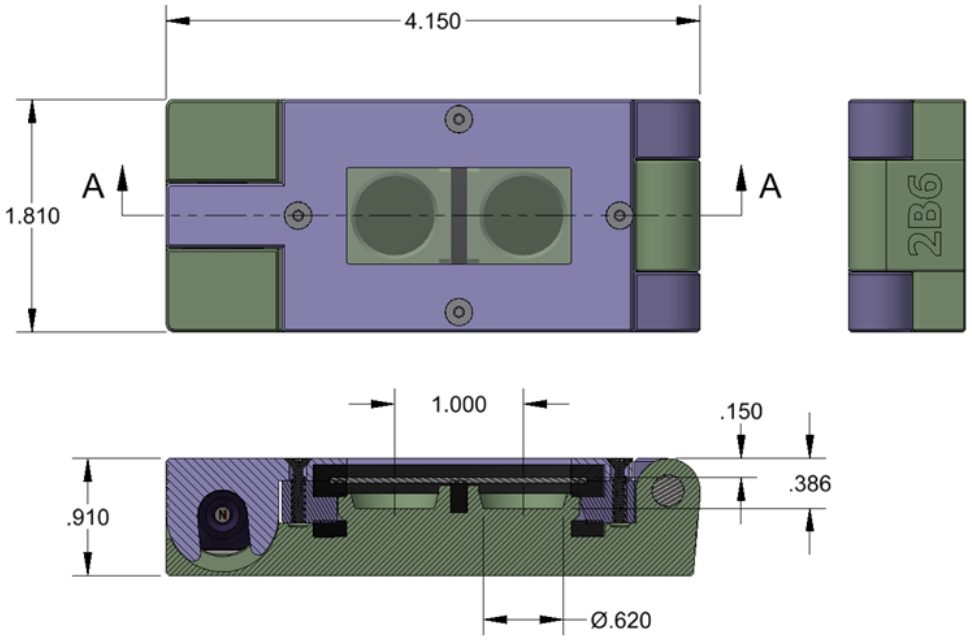

SECTION A-A

Microscope Slide Fixture (MSF) Assembly Instructions – DIMENSIONS OF OPEN FLIPPER
20231122

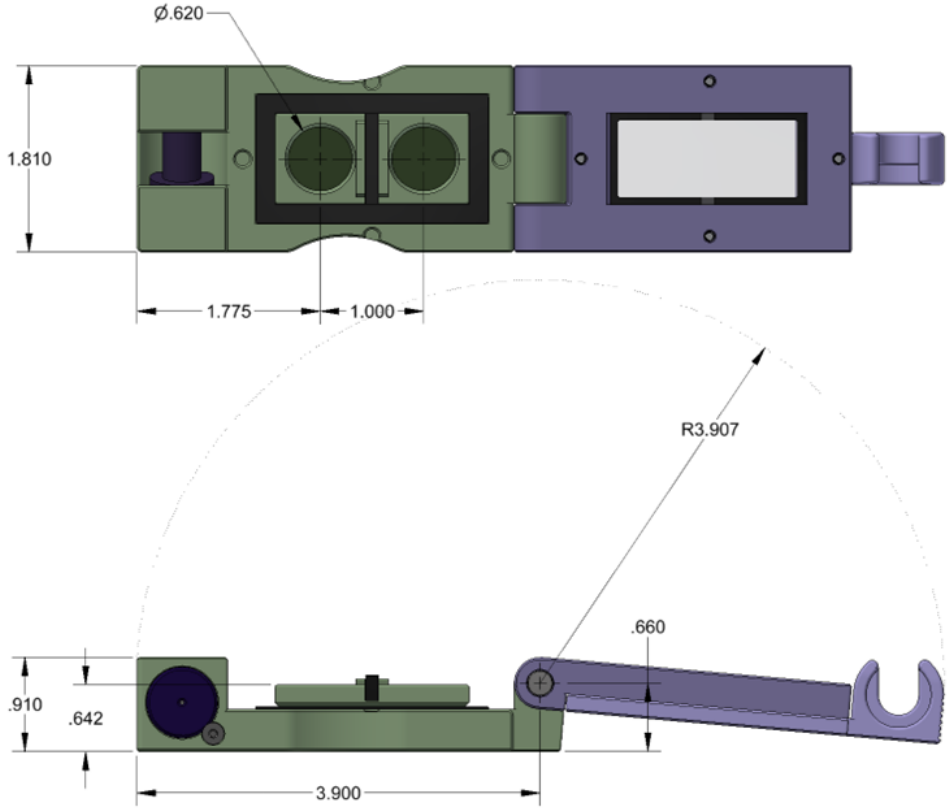

12

Microscope Slide Fixture (MSF) Assembly Instructions – FLIPPER WITH COVER
20240116

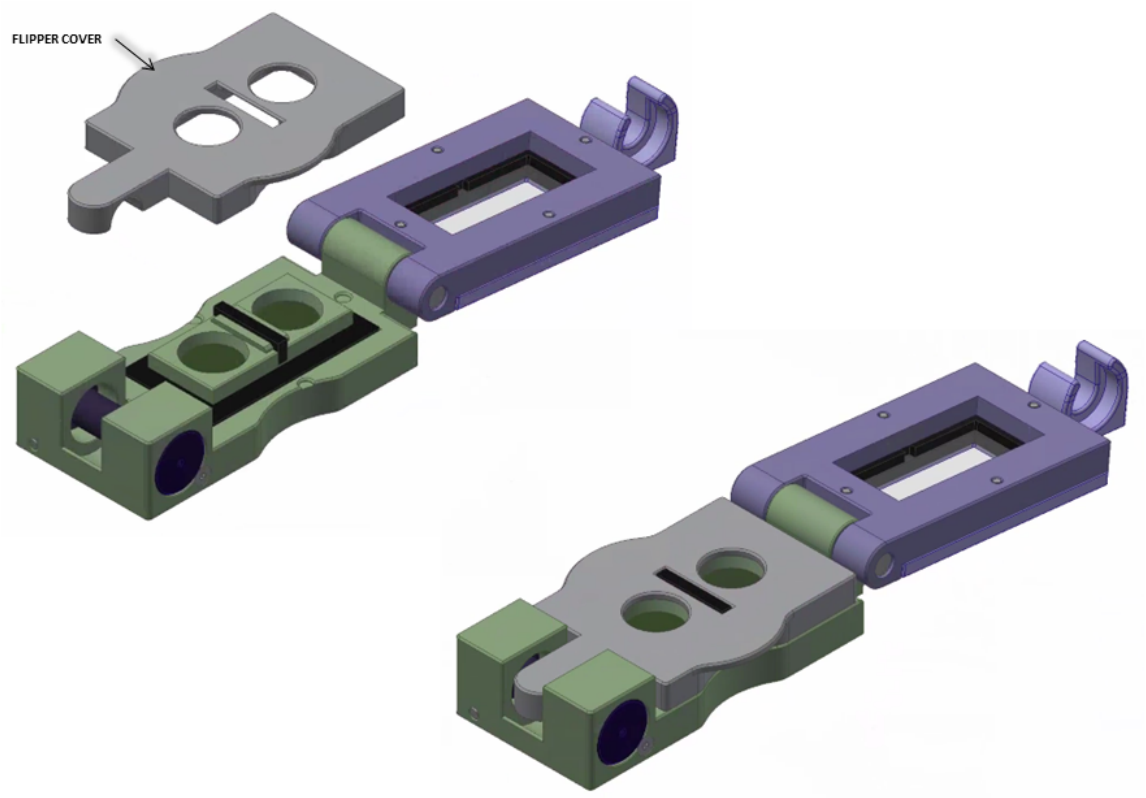

13